

Conserved structural elements in the V3 crown of HIV-1 gp120

Xunqing Jiang^{1,6}, Valicia Burke^{1,6}, Maxim Totrov², Constance Williams³, Timothy Cardozo⁴, Mirosław K Gorny³, Susan Zolla-Pazner^{3,5} & Xiang-Peng Kong¹

Binding of the third variable region (V3) of the HIV-1 envelope glycoprotein gp120 to the cell-surface coreceptors CCR5 or CXCR4 during viral entry suggests that there are conserved structural elements in this sequence-variable region. These conserved elements could serve as epitopes to be targeted by a vaccine against HIV-1. Here we perform a systematic structural analysis of representative human anti-V3 monoclonal antibodies in complex with V3 peptides, revealing that the crown of V3 has four conserved structural elements: an arch, a band, a hydrophobic core and the peptide backbone. These are either unaffected by or are subject to minimal sequence variation. As these regions are targeted by cross-clade neutralizing human antibodies, they provide a blueprint for the design of vaccine immunogens that could elicit broadly cross-reactive protective antibodies.

Only a safe and effective vaccine can halt the global AIDS pandemic, but such a vaccine remains elusive. Identifying structurally conserved immunologic determinants on the surface glycoproteins of HIV-1 can facilitate the design and development of an effective HIV-1 vaccine that will induce protective antibodies^{1–3}. HIV-1 enters human cells by binding, via its envelope glycoprotein gp120, to cell-surface molecules CD4, which acts as a virus receptor, and CCR5 or CXCR4, which acts as alternative virus coreceptors^{4–7}. Binding of HIV-1 to these molecules is mediated by at least two regions on gp120 containing conserved structural elements: the CD4 binding site and the chemokine receptor binding site. The CD4 binding site is composed of several discontinuous structural regions of gp120 (ref. 8); similarly, the chemokine receptor binding site is highly conformational and discontinuous and is composed of the bridging sheet, including the stem of V1V2, and the third variable region (V3) of gp120 (refs. 7–9). The existence of conserved structural elements in the CD4 binding site is commonly recognized¹⁰. However, the V3, as its name implies, has generally been considered to have little conservation, despite extensive evidence to the contrary^{11–21}.

At the sequence level, V3 is more conserved in comparison with the other variable regions of gp120. It has limited variation in length, as it is almost always 35 residues long, and it harbors at its tip a highly conserved motif, Gly-Pro-Gly-Arg/Gln (GPGR/Q, residues 312–315 in the HXB2 numbering scheme²²). These relatively constant elements in V3 were recognized very early by sequence analysis¹⁸.

Structures of V3 have been resolved recently in the context of the CD4-bound gp120 core and alone in complex with human monoclonal antibodies (mAbs) derived from infected individuals^{7,9,23–27}. V3 protrudes ~30 Å from the CD4-bound gp120 core^{7,9}, and this

extended structure can be divided into three regions: the base, the stem and the crown. The conserved base is seated on the gp120 core with a disulfide bridge, whereas the stem extends outwards and is presumably highly flexible⁹. The crown consists of ~13 residues in the center of the V3 sequence and forms a β -conformation at the distal apex.

V3 is highly immunogenic and was named the “principal neutralizing determinant” of HIV-1 (ref. 28). Anti-V3 antibodies are found in the sera of essentially all individuals infected with HIV-1 (refs. 29–34), and a large panel of anti-V3 mAbs has been produced^{34–37}. When tested for neutralizing activity, anti-V3 mAbs have been found to neutralize up to ~50% of the viruses in various multiclade panels^{38–41}. In a recent study⁴², a panel of human anti-V3 mAbs, including 2219, 2557 and 3074, was tested for neutralizing activity against 41 pseudoviruses and was shown to neutralize 24–39% of the pseudoviruses, including tier 1 and tier 2 pseudoviruses from clades A, B and C as well as clade B pseudoviruses derived from chronically infected donors. The range of neutralization of these anti-V3 mAbs is quite compatible with those of two well-known broadly neutralizing mAbs, b12 and 2G12, when tested similarly against 162 pseudoviruses and assessed also on the basis of their IC₅₀ values⁴³. Moreover, the immunization of animals with V3-containing immunogens elicits anti-V3 antibodies^{44–49}. Recently, a novel immunization regimen combining DNA primes and recombinant protein boosts has been shown to focus rabbit immune responses on V3 and elicit antibodies with cross-clade neutralization activity^{45,47}. Furthermore, both monoclonal and polyclonal anti-V3 antibodies show intra- and intersubtype neutralization of diverse HIV strains^{30,38,40,41,50–52}, and human mAbs that target quaternary structure-dependent envelope epitopes composed of regions of V2

¹Department of Biochemistry, New York University School of Medicine, New York, New York, USA. ²Molsoft LLC, La Jolla, California, USA. ³Department of Pathology, New York University School of Medicine, New York, New York, USA. ⁴Department of Pharmacology, New York University School of Medicine, New York, New York, USA. ⁵Veterans Affairs New York Harbor Healthcare System, New York, New York, USA. ⁶These authors contributed equally to this work. Correspondence should be addressed to X.-P.K. (xiangpeng.kong@med.nyu.edu).

Received 22 December 2009; accepted 29 April 2010; published online 11 July 2010; corrected online 21 July 2010; doi:10.1038/nsmb.1861

and V3 tolerate sequence variation in V3 and can have broad neutralizing activity and/or extremely high potency^{43,53,54}. Thus, V3 is well suited as a target for HIV-1 vaccine development². Notably, all of the known human anti-V3 mAbs are against the crown^{19,24,25,27,41,55,56}; thus, the crown can serve as a neutralizing epitope⁵⁷.

One way to identify functionally conserved structural elements is to determine the structures of epitopes bound to anti-HIV-1 human mAbs, especially those with broad reactivity¹⁰. The availability of many anti-V3 human mAbs has made it possible to make structural comparisons of the epitopes they recognize, and this has been performed with four anti-V3 human mAbs (mAbs 447-52D, 537-10D, 2219 and F425-B4e8) in complex with various V3 peptides^{13,24-27}. However, no general pictures of conserved structural elements of V3 have emerged from these structures. Here, we present 10 new crystal structures of the Fab fragments of cross-clade neutralizing human anti-V3 mAbs 2557, 1006-15D and 3074, as well as that of a strain-restricted mAb 268-D, in complex with V3 peptides derived from various HIV-1 strains and with a circularly-permuted V3 mimotope that preserves specific structural elements. The systematic crystallographic structure determination of these complexes has led to the identification of conserved structural elements in the V3 crown and their interactions with human antibodies. These elements can be used for the development of immunogens designed to elicit broadly reactive, cross-clade neutralizing antibodies.

RESULTS

2557 recognizes conserved structural elements of the V3 crown

We derived human anti-V3 mAb 2557 (IgG1 λ) from the blood cells of an individual from Cameroon infected with CRF02_AG HIV-1. The mAb reacts strongly with V3 from subtypes A and B expressed as fusion proteins on a truncated form of MuLV gp70, and in several types of assays, it neutralizes a number of viruses from clades A, B and C^{42,57,58}. We determined the crystal structures of the Fab fragment of mAb 2557 (Fab 2557) in complex with four different V3 peptides with divergent residue sequences derived from HIV-1 strains of subtypes A, B and C (Fig. 1, Table 1, Supplementary Fig. 1 and Supplementary Table 1).

All four peptides in complex with Fab 2557 form a β -hairpin structure (Fig. 1b,c); they lie across a binding groove surrounded by the complementarity-determining regions (CDRs) of both light and heavy chains of the mAb (Fig. 1b and Supplementary Fig. 1). The binding

groove is roughly shaped like a cradle ~ 7 Å deep, so that the entire V3 crown sinks into the binding site.

The V3 structure in complex with Fab 2557 can be naturally divided by its interactions with the CDRs into three regions: the arch (V3 residues 312–315), the circllet (residues 306–309, 316 and 317) and the band (residues 304–305 and 318) (Fig. 1). The arch interacts preferentially with CDR L1, the circllet with CDR L3 on one side and CDR H3 on the other side and the band with CDR H1 and H2 (Fig. 1b). The arch that harbors the highly conserved GPGR/Q motif is at the apex of the V3 crown. It forms a β -turn, and its GPG corner rests snugly on the backbone between residues Lys^{L31} and Tyr^{L32} of CDR L1 (L in the superscript refers to the light chain) and stacks against the side chain of Tyr^{L32} (Fig. 2a). The side chain of V3 residue 315, which alternates between arginine and glutamine in more than 90% of HIV-1 strains, points away from mAb 2557 (Figs. 1b and 2a). Hence, this residue does not have an important role in antigen-antibody interaction in mAb 2557–V3 complexes and does not limit the neutralizing activity to subtype B, which predominantly carries a GPGR arch, or to non-B strains that predominantly carry GPGQ^{20,40}.

The circllet, the central region of the V3 crown, presents more diverse sequences in HIV-1 strains than those of the arch and band regions (Fig. 1a,c; see also below) and has two sides, one facing CDR L3 and the other facing CDR H3 (Fig. 1b). The side facing CDR L3 (i) is made of the side chains of residues 307, 309 and 317, three highly conserved V3 positions²⁰, (ii) forms a hydrophobic core of the V3 crown (Fig. 1b,c) and (iii) interacts with a hydrophobic region of the antibody formed by CDR L3 residues, including Trp^{L91}, Ala^{L93} and Leu^{L98}. Here, the indole ring of Trp^{L91} lies flat at the base of the binding pocket (Fig. 1b). In contrast, the side of the circllet facing CDR H3 is made of the side chains of residues 306, 308 and 316. These three residues are variable in HIV-1 strains and are often hydrophilic²⁰.

The band of the V3 crown consists of residues 304 and 305 of the N-terminal strand and residue 318 on the C-terminal strand (Figs. 1 and 2). The interaction between the V3 band and Fab 2557 has two components. First, the side chains of its basic residues Arg³⁰⁴ and Lys³⁰⁵ form potential salt bridges with the side chains of three acidic residues, Asp^{H31}, Asp^{H54} and Asp^{H56} (H in the superscript refers to the heavy chain) from CDR H1 and H2 (Figs. 1b and 2c). Second, the extended side chain of Lys³⁰⁵ is sandwiched between the phenyl rings of Tyr^{H52} from CDR H2 and residue Tyr³¹⁸ of the V3 itself (Fig. 2c).

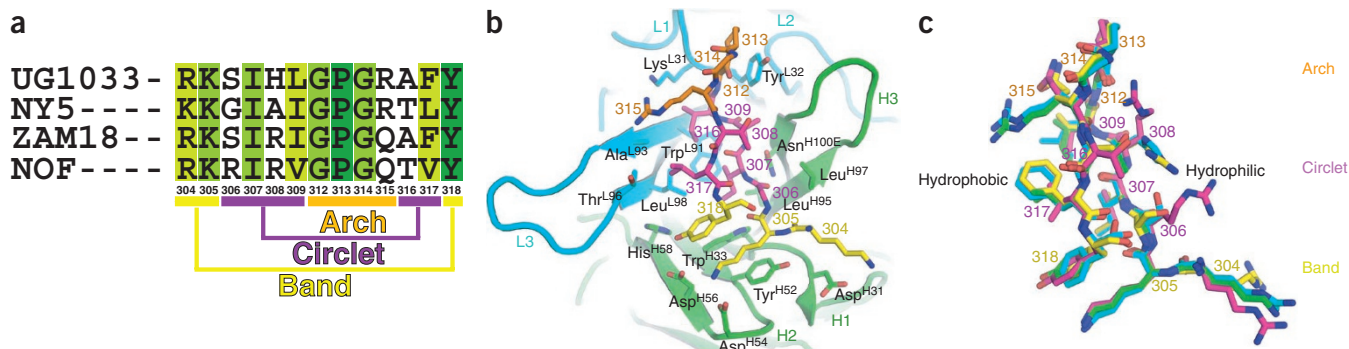


Figure 1 The three regions of the V3 crown as revealed by the structure of Fab 2557 in complex with four V3 peptides. (a) Sequence alignment of four V3 peptides (from the viruses named on the left) that were complexed with Fab 2557. Residues are numbered in the HXB2 numbering scheme²², and the three regions of the crown are indicated below the sequences. The intensity of the green color in the sequence alignment corresponds to degree of sequence conservation at that position. (b) NY5 V3 peptide in complex with Fab 2557. The light chain (cyan) and heavy chain (green) are shown as ribbons, and antibody residues that have an epitope contact area comprising more than 10 Å² of their accessible surface are shown as sticks. The arch, circllet and band of the V3 crown are colored orange, magenta and yellow, respectively. (c) Structural superimposition of the four peptides that were crystallized in complex with Fab 2557. The carbon atoms of the four peptides are colored cyan (UG1033), green (NY5), magenta (NOF) and yellow (ZAM18). The three regions of the V3 crown and the hydrophobic and hydrophilic sides of the circllet are indicated.

Table 1 Data collection and refinement statistics

	Fab 2557–NY5	Fab 2557–UG1033	Fab 2557–NOF	Fab 2557–ZAM18	Fab 2557–V3 mimotope	Fab 1006–15D–MN	Fab 3074–V1191	Fab 3074–UR29	Fab 3074–MN	Fab 268–D–MN
Data collection										
Space group	<i>P</i> 1	<i>P</i> 2 ₁	<i>P</i> 1	<i>P</i> 1	<i>C</i> 2	<i>C</i> 2	<i>P</i> 6 ₅ 22	<i>P</i> 2 ₁	<i>P</i> 2 ₁	<i>P</i> 2 ₁
Cell dimensions										
<i>a</i> , <i>b</i> , <i>c</i> (Å)	42.41, 43.08, 58.21	75.68, 142.93, 85.01	42.55, 42.74, 116.06	42.45, 43.17, 57.82	168.75, 43.05, 274.34	98.92, 82.31, 149.83	100.45, 100.45, 177.74	59.95, 128.79, 60.10	59.87, 128.79, 60.10	46.38, 69.26, 71.69
α , β , γ (°)	87.86, 85.51, 85.82	90.00, 95.00, 90.00	87.91, 85.20, 85.98	89.16, 86.25, 85.19	90.00, 94.21, 90.00	90.00, 110.35, 90.00	90.00, 90.00, 120.00	90.00, 92.54, 90.00	90.00, 92.66, 90.00	90.00, 107.24, 90.00
Resolution (Å)	1.8 (1.86–1.8)	2.5 (2.59–2.5)	2.5 (2.59–2.5)	2.8 (2.9–2.8)	2.5 (2.54–2.5)	2.7 (2.8–2.7)	3.0 (3.11–3.0)	1.7 (1.76–1.70)	1.9 (1.97–1.90)	1.9 (1.96–1.90)
<i>R</i> _{sym} (%)	5.3 (13.1)	4.7 (31.1)	12.2 (36.4)	11.2 (35.2)	7.8 (31.8)	15.6 (36.3)	16.2 (49.4)	7.6 (23.6)	13.8 (36.9)	7.7 (26.2)
<i>I</i> / σ <i>I</i>	24.9 (12.9)	17.2 (2.0)	10.2 (3.7)	11.7 (4.2)	17.6 (4.6)	9.25 (2.1)	24.8 (9.1)	19.6 (4.3)	16.6 (2.7)	23.1 (5.3)
Completeness (%)	97.6 (96.3)	99.9 (100)	90.3 (90.1)	98.8 (98.3)	90.9 (70.7)	94.0 (71.2)	100 (100)	96.9 (91.0)	96.5 (86.3)	99.0 (97.4)
Redundancy	3.9 (4.0)	4.3 (4.3)	3.6 (3.7)	3.9 (3.9)	4.1 (3.8)	4.8 (3.7)	23.2 (24.0)	4.3 (4.1)	6.9 (5.7)	7.5 (5.9)
Refinement										
Resolution (Å)	1.8	2.5	2.5	2.8	2.5	2.7	3.0	1.7	1.9	1.9
No. reflections	37,562	62,523	25,771	10,107	60,726	29,059	11,277	94,853	67,118	32,721
<i>R</i> _{work} / <i>R</i> _{free}	18.1 / 21.6	20.2 / 28.0	23.4 / 29.3	21.2 / 29.1	21.6 / 27.4	21.8 / 28.3	21.6 / 30.8	20.4 / 22.3	19.1 / 22.6	19.1 / 21.3
No. atoms										
Protein	3,448	13,300	6,842	3,411	13,937	6,979	3,477	6,836	6,784	3,359
Ligand/ion	–	–	–	–	–	30	–	–	–	25
Water	479	328	434	123	709	161	188	879	751	351
<i>B</i> -factors										
Protein	12.96	44.36	19.43	33.78	28.27	48.06	47.19	17.97	25.89	26.01
Ligand/ion	–	–	–	–	–	90.61	–	–	–	46.25
Water	22.47	34.63	21.96	20.38	23.08	39.34	33.75	26.59	32.37	36.20
R.m.s. deviations										
Bond lengths (Å)	0.005	0.007	0.007	0.008	0.006	0.007	0.006	0.005	0.005	0.007
Bond angles (°)	1.421	1.422	1.498	1.527	1.389	1.58	1.4	1.4	1.44	1.1

Values in parentheses are for highest-resolution shells.

This π -cation stacking is supported from below by Trp^{H33} from CDR H1. Therefore, Lys305 is well coordinated by the antibody through several specific interactions. Notably, mAb 2557 has an unusually long CDR L3 (19 residues), but it points away from the V3 binding site; only residues at its base make contacts with V3 (Fig. 1b).

Other mAbs bind V3 similarly to mAb 2557

The antigen-antibody interactions of mAb 2557 are highly similar to those previously determined for human mAb 2219–V3 complexes²⁵. The importance of this similarity is underscored by the fact that mAb 2557 was produced by the cells of an individual infected with CRF02_AG in Cameroon, whereas mAb 2219 was selected from the cells of an individual infected with clade B in the US. In particular, the arch- and band-specific interacting residues, including Tyr^{L32}, Trp^{L91}, Asp^{H31}, Asp^{H54}, Asp^{H56}, Tyr^{H52} and Trp^{H33}, are identical between these two antibodies (Supplementary Fig. 2). Moreover, the three structural regions observed in complexes formed by Fab 2557 with four different V3 peptides are also observed with the mAb 2219–V3 structures²⁵ (Fig. 2a,c and Supplementary Fig. 3). This suggested that other human mAbs that harbor these residues might also interact with V3 in the same manner. In fact, we found that human anti-V3 mAb 1006-15D (IgG1 λ) (mAb 1006), derived from a North American individual infected with a clade B virus, also has identical residues at these positions (Supplementary Fig. 2).

To investigate whether mAb 1006 has a mode of antigen-antibody interactions similar to that of mAbs 2219 and 2557, we determined the crystal structure of its Fab fragment in complex with the V3 peptide

from the clade B strain MN (Fig. 2b,d, Table 1, Supplementary Fig. 1 and Supplementary Table 1). This structure showed that the interaction of Fab 1006 with V3 is indeed extremely similar to those of Fabs 2219 and 2557 (Fig. 2b,d and Supplementary Fig. 4). In particular, the tyrosine stacking with the arch, salt bridges with the basic residues of the band and the π -cation sandwich of the side chain of residue Tyr318 in the band are all conserved in mAb 1006 (Fig. 2b,d). These data suggest that mAbs 2557, 2219 and 1006, derived from individuals infected in the US and Cameroon with different strains of HIV from different subtypes, all belong to a ‘family’ of antibodies that recognize V3 using similar modes of binding.

3074 focuses on the hydrophobic core of the crown

Human anti-V3 mAbs 1006, 2219 and 2557 show neutralizing activity against viruses from several subtypes^{11,12,42,57,58}. Our data show that the structural basis of their broad reactivity rests on their interaction with structural elements in V3 that are relatively constant: the arch, the band and the hydrophobic face of the circlet. To determine if recognition of these elements applies to other broadly reactive human anti-V3 mAbs, we determined the crystal structures of the Fab fragment of another cross-clade neutralizing human mAb, 3074, in complex with three V3 peptides (Fig. 3, Table 1, Supplementary Fig. 1 and Supplementary Table 1). We derived human mAb 3074 (IgG1 λ) from another individual infected with CRF02_AG HIV-1 in Cameroon. It neutralizes several primary HIV-1 isolates and reacts broadly with pseudoviruses expressing V3 derived from several different subtypes^{42,58}.

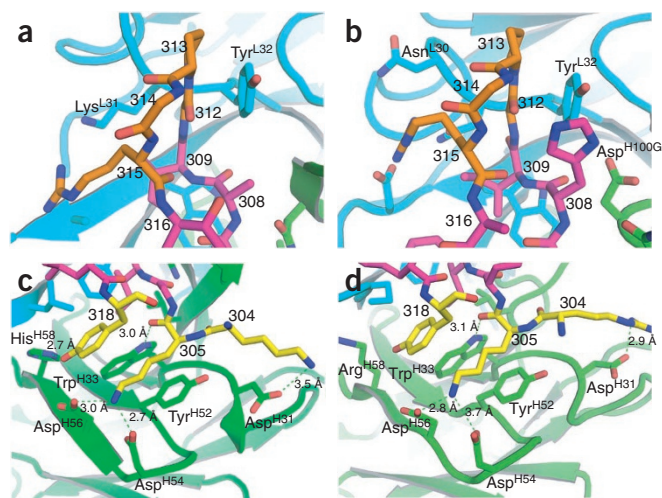
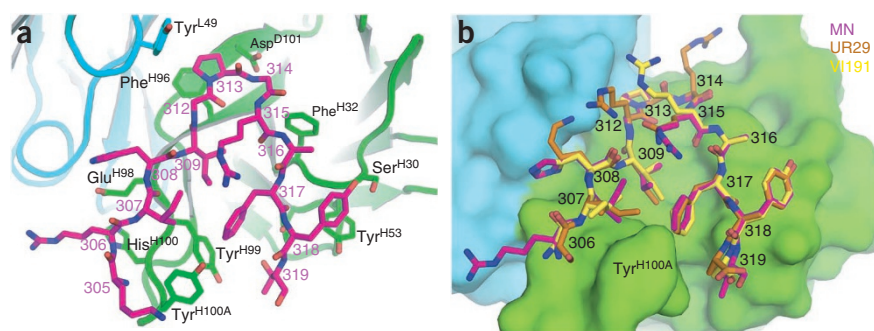


Figure 2 Conserved binding mode of human mAbs 1006 and 2557. (a,b) Fab 2557 (a) and Fab 1006 (b) bind to the V3 arch region (orange) by stacking the GPG turn against a conserved Tyr^{L32}. (c,d) Fab 2557 (c) and Fab 1006 (d) bind to the V3 band region (yellow) by salt bridges and π -cation stacking using conserved residues. The structure of human mAb 2219, published previously²⁵, shows the same antigen-binding mode (Supplementary Fig. 3).

Human Fab 3074 binds V3 in a mode that differs from the other anti-V3 human mAbs that have been studied structurally but uses the same basic V3 elements we have identified. First, like the broadly reactive human mAb 447-52D²⁴, peptide backbone interactions between V3 and Fab 3074, which are generally less perturbed by residue variation, are prominent (Fig. 3a and Supplementary Fig. 5). The N-terminal strand of the V3 forms three main chain hydrogen bonds with the backbone of CDR H3, forming a three-stranded β -sheet with CDR H3 (Supplementary Fig. 5). Second, the V3 crown complexed to Fab 3074 is no longer a near-ideal antiparallel β -hairpin but is distorted and shaped like the letter A (Fig. 3 and Supplementary Fig. 5a). Although the arch is still a rather tight turn, the two strands are split by the protruding side chain of CDR H3 residue Tyr^{H100A}, which wedges into the band region of the V3 crown (Fig. 3b). This splitting of the cirlet and band of the V3 crown causes the side chains of the three hydrophobic residues of the cirlet region, at positions 307, 309 and 317, to lie approximately on a plane (Supplementary Fig. 5b). However, these residues are still able to contact each other (forming the central link between the legs of the letter A; Supplementary Fig. 5a) and create an extended hydrophobic surface. Notably, Pro³¹³ of the arch forms a π -stacking with Phe^{H96}, aided on the side by Tyr^{L49} (Fig. 3a). Thus, overall, the broadly reactive mAb 3074 interacts with V3 through three

Figure 3 Fab 3074 in complex with three V3 peptides. (a) MN V3 peptide in complex with Fab 3074. (b) Structural superimposition of three peptides of viral strains MN, UR29 and V1191 that were crystallized with Fab 3074. The Fab fragment is shown as a protein surface. Note that Tyr^{H100A} of CDR H3 wedges into the V3 band region, flattening out the hydrophobic core formed by the highly conserved V3 residues at positions 307, 309 and 317 to form an extended hydrophobic surface (see also Supplementary Fig. 5).



conserved V3 structural elements: the V3 main chain, the hydrophobic core and the arch via a π -stacking of the GPG turn. All of these are either unaffected by sequence or are not subject to sequence variation.

Strain-restricted mAb 268-D is side chain specific

To investigate whether (and if so, how) the binding of broadly reactive anti-V3 mAbs differs from that of strain-specific, narrowly reactive anti-V3 mAbs, we determined the crystal structure of the MN V3 peptide in complex with the Fab fragment of mAb 268-D (Fig. 4, Table 1, Supplementary Fig. 1 and Supplementary Table 1), whose neutralizing activity is quite narrow¹⁹. We derived human mAb 268-D (IgG1 λ) from an individual from the US infected presumably with a clade B virus. The mAb was selected with a 23-mer V3 peptide of the MN strain⁴⁰, and its binding and neutralizing capacity is limited to HIV-1 strain MN¹⁹. The most striking feature of the Fab 268-D-V3 complex is that the antigen-binding site of this antibody binds predominantly to the side chains of three basic residues of the V3 crown: Lys³⁰⁵, His³⁰⁸ and Arg³¹⁵ (Fig. 4). These three residues contribute ~60% of the contact areas between the mAb and the V3 epitope. Moreover, there is a surface binding pocket specific for each of these three side chains (Fig. 4b). The Lys³⁰⁵-binding pocket is formed by residues from CDR L1 and L2, with Asp^{L51} placed at the bottom of this pocket so that it can form a salt bridge with Lys³⁰⁵ (Fig. 4a). The His³⁰⁸ binding pocket is formed by residues from both light and heavy chain CDRs, and 65% of the surface area of His³⁰⁸ is buried in the pocket. The Arg³¹⁵ binding pocket is also highly specific for this basic residue: there are several negatively charged residues in the heavy chain near this binding pocket, and Glu^{H95} and Asp^{H100A} can form salt bridges with Arg³¹⁵ (Fig. 4a). Of these two negatively charged residues, Glu^{H95} is completely buried by V3 binding. The narrow specificity of mAb 268-D and its targeting of Arg³¹⁵ extends previous data showing that mAbs that engage Arg³¹⁵ are essentially restricted in their neutralizing activity to viruses, primarily from clade B, with the GPGR, rather than GPGQ, motif at the tip of the loop^{25,26,38,49,56}. In contrast, anti-V3 mAbs for which binding to residue Arg/Gln³¹⁵ is not essential (for example, mAbs 2219, 2557, 1006 and 3074) can show cross-clade neutralizing activities.

As V3 residues Lys³⁰⁵, His³⁰⁸ and Arg³¹⁵ are among the most variable residues in the V3 crown (see below), specificity for their side chains makes mAb 268-D highly strain specific. This is in direct contrast to the binding mode of the broadly reactive mAbs 2219, 2257, 1006 and 3074, which engage the four areas (backbone, arch, band and hydrophobic face of the cirlet) that are minimally perturbed by sequence substitution. In fact, mAb 268-D binds V3 on the opposite face from that of the broadly reactive mAb 3074 (Supplementary Fig. 6). Notably, our structure of Fab 268-D also reveals the structural basis for why this mAb can react with a non-V3 hexapeptide (Supplementary Fig. 7).

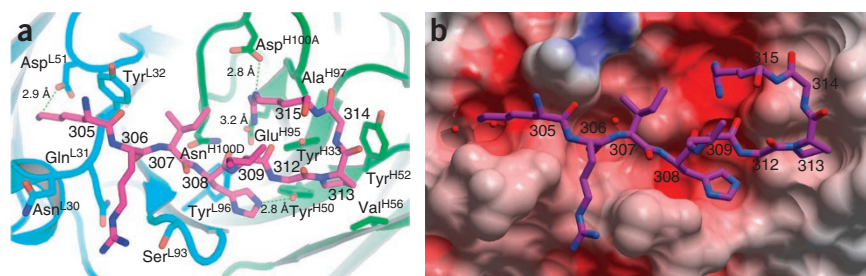


Figure 4 Sequence-specific binding of Fab 268-D to MN V3 peptide. (a) MN V3 peptide in complex with Fab 268-D. Note that Lys305 of V3 forms a salt bridge with Asp^{L51}, and Arg315 of V3 with Glu^{H95} and Asp^{H100A}. (b) Side chain-specific binding pockets on mAb 268-D. Here Fab 268-D is shown as a protein surface colored according to its electrostatic potentials.

in the cases of mAbs 3074 and 447-52D), form the four conserved structures of the V3 crown (Fig. 5a). These are bound by broadly reactive anti-V3 antibodies. In contrast, antibodies such as 268-D that bind to nonconserved surfaces are strain restricted and relatively narrow or have type-specific reactivity. Thus, the combination of elements that an antibody recognizes will determine the limits or breadth of its cross-reactivity. Moreover, the sequence variability of the hydrophilic face of the circlet suggests that this face may be the ‘anti-hotspot’ predicted to exist in V3 that sometimes camouflages the functional, conserved receptor binding site⁸.

Structural elements of V3

Taken together, our data show that the HIV-1 V3 crown can be divided into distinct regions containing several structural elements and that broadly reactive anti-V3 mAbs bind to these conserved elements: the arch, the circlet, the band and the V3 peptide main chain backbone (Fig. 5a). This is further illustrated by the overlay of residue sequences found in the crown (Fig. 5b). The arch is the apex β -turn of the crown, consisting of the highly conserved GPGR/Q motif. The circlet is the middle region of the V3 crown with a hydrophilic face and a hydrophobic face. Three residues on the hydrophobic face, residues 307 and 309 (very often two isoleucines) and 317 (often a phenylalanine), form the hydrophobic ‘core’ of the V3 crown. The hydrophilic face contains residue 308 (often an arginine or a histidine), N-terminal residue 306 (often a serine) and the C-terminal residue 316 (usually an alanine or a threonine). The band region is formed by the often positively charged residues 304 and 305 (usually an arginine and a lysine, respectively) and residue 318 (usually a tyrosine). Data supporting the conserved nature of these regions comes from sequence analyses from early and current studies which reveal that residues that constitute the ³¹²GPG³¹⁴ of the arch, the three residues in the hydrophobic core (for example, Ile307, Ile309 and Phe317) and the three residues in the band (for example, Arg304, Lys305 and Tyr318) are relatively more conserved compared to other positions in V3 (refs. 18,20). These elements, together with the V3 peptide backbone, which can form main chain interactions (as

A mimotope presents the conserved structural elements

One method that can assess structural elements as determinants for antigen-antibody interaction is circular permutation, an approach that has been used in protein engineering to identify structural cores of protein folding and essential functional elements in enzymes^{59–61}. With this in mind, we designed a V3 mimotope with the following residue sequence: AC-QAFY-ASSP-RKSIHIG-ACA (Fig. 5c, inset, and Supplementary Fig. 8a), which is a cyclic peptide that retains the N- and C-terminal sequences of V3 (underlined). In this mimotope, the GPG motif of the V3 arch is replaced with a disulfide bond, and the open end of the hairpin is bridged with a four-residue linker, Ala-Ser-Ser-Pro. The linker was designed to preserve the spatial relationship of the N- and C-terminal strands by a combination of knowledge-based and energy-minimization approaches (see Online Methods). The resulting mimotope peptide preserved the key structural elements in the circlet and band regions of V3. ELISA data show that this mimotope interacts with the family of broadly reactive mAbs 1006, 2219 and 2557 but not with mAbs like 447-52D and 268-D, which are dependent on interaction with Arg315 in the arch (Supplementary Table 2). A 2.5-Å resolution crystal structure of this mimotope in complex with the Fab fragment of mAb 2557 shows that the mimotope interacts with Fab 2557 in the same manner as does a native V3 epitope (that is, through the hydrophobic core and the band) (Fig. 5c, Table 1 and Supplementary Fig. 8).

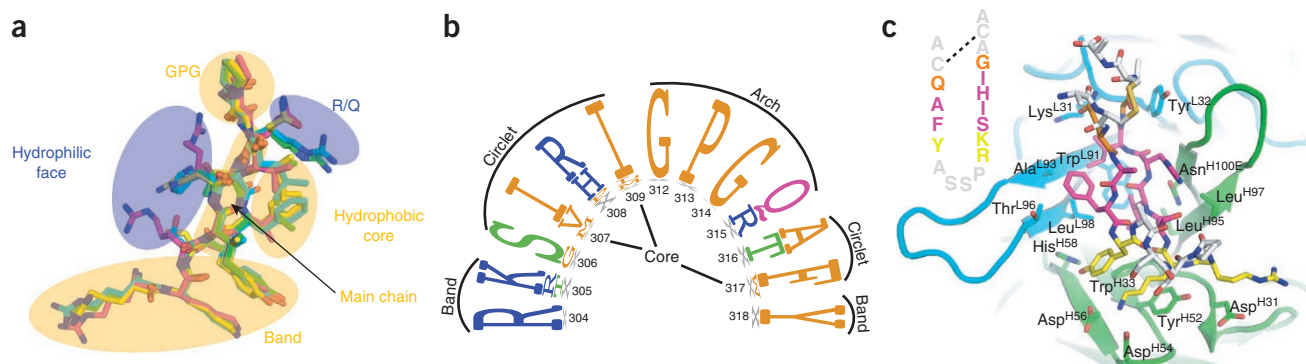


Figure 5 Conserved structural elements of V3. (a) The four conserved V3 elements, visualized from the antibody side and highlighted in light orange, are the GPG turn of the arch, the hydrophobic core in the circlet, the band and the backbone that can interact with mAbs by main chain interactions. Two variable regions that limit antibody cross-reactivity are highlighted in blue: the hydrophilic face in the circlet and the arginine/glutamine residue in the arch. (b) Sequence conservation of the V3 crown. The height of the residues at each V3 position is proportional to its frequency of distribution in clades A, B and C²⁰. The residue numbering and their participation in the arch, hydrophobic core and band are indicated. (c) A V3 mimotope, generated by circular permutation, in complex with Fab 2557. The structure of the complexed mimotopes is similar to that of V3 peptides complexed with Fab 2557 shown in Figure 1. V3 residues are colored orange (arch), magenta (circlet) and yellow (band), whereas the additional residues introduced by circular permutation are colored gray. Inset, sequence of the mimotope. Note that the mimotope binds the mAbs in the same mode as V3 (see Fig. 1b and Supplementary Fig. 8).

DISCUSSION

The identification of conserved structural elements in V3 may serve as a blueprint for immunogens designed to overcome the antigenic diversity of V3. Immunogens designed to focus the immune system on V3 epitopes in the backbone, arch, band and/or hydrophobic face of the circlet should elicit broad rather than type-specific neutralizing antibodies, helping to circumvent the virus's troublesome antigenic diversity. Our artificial V3 mimotope provides an example of a rationally designed mimotope that can potentially focus the immune response on structurally conserved elements. Indeed, understanding the relationship between sequence variation and three-dimensional structural conservation should provide a blueprint for the design of immunogens that will induce antibodies to V3 and other variable regions of gp120 that are known to induce potent neutralizing antibodies^{2,43,53,62}. Moreover, the use of similar approaches to identify structurally conserved elements in other antigenically diverse human pathogens should similarly contribute to the design of vaccines with broad efficacy against pathogens characterized by a multitude of strains.

METHODS

Methods and any associated references are available in the online version of the paper at <http://www.nature.com/nsmb/>.

Accession codes. Protein Data Bank: Coordinates and structure factors for the Fab complexes have been deposited with the following accession codes: 3GO1 (Fab 268-D-MN V3), 3MLR (Fab 2557-NY5), 3MLS (Fab 2557-mimotope), 3MLT (Fab 2557-UG1033), 3MLU (Fab 2557-ZAM18), 3MLV (Fab 2557-NOF), 3MLW (Fab 1006-MN), 3MLX (Fab 3074-MN), 3MLY (Fab 3074-UR29) and 3MLZ (Fab 3074-VI191).

Note: Supplementary information is available on the Nature Structural & Molecular Biology website.

ACKNOWLEDGMENTS

We thank R. Allison, formerly Press Secretary to Queen Elizabeth II, for providing the definition of the regions of the crown, as exemplified by the St. Edward's crown worn by Edward the Confessor, J. Sampson for assisting with the structure refinement and figure preparation, T. O'Neal and X.-H. Wang for antibody production and sequence analysis, staff members at beamlines X4A, X4C and X6A at the National Synchrotron Light Source for X-ray diffraction data collections and C. Hioe and N. Cowan for critical comments on the work and manuscript. This study was supported in part by the Bill and Melinda Gates Foundation, US National Institutes of Health grants AI36085 and HL59725, the Immunology Core of the New York University Center for AIDS Research (US National Institutes of Health grant AI27742) and by research funds from the US Department of Veterans Affairs.

AUTHOR CONTRIBUTIONS

X.J. and V.B. crystallized the complexes and collected the X-ray data; M.T. designed the V3 mimotope; C.W. produced the mAbs; T.C., M.K.G., S.Z.-P. and X.-P.K. designed the experiments; S.Z.-P. and X.-P.K. wrote the manuscript; all authors discussed the results and commented on the manuscript.

COMPETING FINANCIAL INTERESTS

The authors declare no competing financial interests.

Published online at <http://www.nature.com/nsmb/>.

Reprints and permissions information is available online at <http://npg.nature.com/reprintsandpermissions/>.

1. Douek, D.C., Kwong, P.D. & Nabel, G.J. The rational design of an AIDS vaccine. *Cell* **124**, 677–681 (2006).
2. Zolla-Pazner, S. Identifying epitopes of HIV-1 that induce protective antibodies. *Nat. Rev. Immunol.* **4**, 199–210 (2004).
3. Montefiori, D., Sattentau, Q., Flores, J., Esparza, J. & Mascola, J. Antibody-based HIV-1 vaccines: recent developments and future directions. *PLoS Med.* **4**, e348 (2007).

4. Feng, Y., Broder, C.C., Kennedy, P.E. & Berger, E.A. HIV-1 entry cofactor: functional cDNA cloning of a seven-transmembrane, G protein-coupled receptor. *Science* **272**, 872–877 (1996).
5. Dragic, T. *et al.* HIV-1 entry into CD4⁺ cells is mediated by the chemokine receptor CC-CKR-5. *Nature* **381**, 667–673 (1996).
6. Deng, H. *et al.* Identification of a major co-receptor for primary isolates of HIV-1. *Nature* **381**, 661–666 (1996).
7. Huang, C.C. *et al.* Structures of the CCR5 N terminus and of a tyrosine-sulfated antibody with HIV-1 gp120 and CD4. *Science* **317**, 1930–1934 (2007).
8. Kwong, P.D. *et al.* Structure of an HIV gp120 envelope glycoprotein in complex with the CD4 receptor and a neutralizing human antibody. *Nature* **393**, 648–659 (1998).
9. Huang, C.C. *et al.* Structure of a V3-containing HIV-1 gp120 core. *Science* **310**, 1025–1028 (2005).
10. Zhou, T. *et al.* Structural definition of a conserved neutralization epitope on HIV-1 gp120. *Nature* **445**, 732–737 (2007).
11. Gorny, M.K. *et al.* Human monoclonal antibodies to the V3 loop of HIV-1 with intra- and interclade cross-reactivity. *J. Immunol.* **159**, 5114–5122 (1997).
12. Gorny, M.K. *et al.* Human monoclonal antibodies specific for conformation-sensitive epitopes of V3 neutralize human immunodeficiency virus type 1 primary isolates from various clades. *J. Virol.* **76**, 9035–9045 (2002).
13. Sharon, M. *et al.* Alternative conformations of HIV-1 V3 loops mimic β hairpins in chemokines, suggesting a mechanism for coreceptor selectivity. *Structure* **11**, 225–236 (2003).
14. Rosen, O., Sharon, M., Quadt-Akabayov, S.R. & Anglistter, J. Molecular switch for alternative conformations of the HIV-1 V3 region: implications for phenotype conversion. *Proc. Natl. Acad. Sci. USA* **103**, 13950–13955 (2006).
15. Cardozo, T. *et al.* Structural basis for coreceptor selectivity by the HIV type 1 V3 loop. *AIDS Res. Hum. Retroviruses* **23**, 415–426 (2007).
16. Cardozo, T. *et al.* Worldwide distribution of HIV type 1 epitopes recognized by human anti-V3 monoclonal antibodies. *AIDS Res. Hum. Retroviruses* **25**, 441–450 (2009).
17. Hartley, O., Klasse, P.J., Sattentau, Q.J. & Moore, J.P. V3: HIV's switch-hitter. *AIDS Res. Hum. Retroviruses* **21**, 171–189 (2005).
18. LaRosa, G.J. *et al.* Conserved sequence and structural elements in the HIV-1 principal neutralizing determinant. *Science* **249**, 932–935 (1990).
19. Gorny, M.K., Xu, J.-Y., Karwowska, S., Buchbinder, A. & Zolla-Pazner, S. Repertoire of neutralizing human monoclonal antibodies specific for the V3 domain of HIV-1 gp120. *J. Immunol.* **150**, 635–643 (1993).
20. Kuiken, C.L. *et al.* *Human Retroviruses and AIDS 1999: A Compilation and Analysis of Nucleic Acid and Amino Acid Sequences* (Theoretical Biology and Biophysics Group, Los Alamos National Laboratory, Los Alamos, New Mexico, USA, 1999).
21. Basmaciogullari, S., Babcock, G.J., Van Ryk, D., Wojtowicz, W. & Sodroski, J. Identification of conserved and variable structures in the human immunodeficiency virus gp120 glycoprotein of importance for CXCR4 binding. *J. Virol.* **76**, 10791–10800 (2002).
22. Ratner, L. *et al.* Complete nucleotide sequences of functional clones of the AIDS virus. *AIDS Res. Hum. Retroviruses* **3**, 57–69 (1987).
23. Dhillon, A.K. *et al.* Structure determination of an anti-HIV-1 Fab 447–52D-peptide complex from an epitaxially twinned data set. *Acta Crystallogr. D Biol. Crystallogr.* **64**, 792–802 (2008).
24. Stanfield, R.L., Gorny, M.K., Williams, C., Zolla-Pazner, S. & Wilson, I.A. Structural rationale for the broad neutralization of HIV-1 by human monoclonal antibody 447–52D. *Structure* **12**, 193–204 (2004).
25. Stanfield, R.L., Gorny, M.K., Zolla-Pazner, S. & Wilson, I.A. Crystal structures of human immunodeficiency virus type 1 (HIV-1) neutralizing antibody 2219 in complex with three different V3 peptides reveal a new binding mode for HIV-1 cross-reactivity. *J. Virol.* **80**, 6093–6105 (2006).
26. Burke, V. *et al.* Structural basis of the cross-reactivity of genetically related human anti-HIV-1 mAbs: implications for design of V3-based immunogens. *Structure* **17**, 1538–1546 (2009).
27. Bell, C.H. *et al.* Structure of antibody F425–B4e8 in complex with a V3 peptide reveals a new binding mode for HIV-1 neutralization. *J. Mol. Biol.* **375**, 969–978 (2008).
28. Javaherian, K. *et al.* Principal neutralizing domain of the human immunodeficiency virus type 1 envelope protein. *Proc. Natl. Acad. Sci. USA* **86**, 6768–6772 (1989).
29. Carrow, E.W. *et al.* High prevalence of antibodies to the gp120 V3 region principal neutralizing determinant of HIV-1MN in sera from Africa and the Americas. *AIDS Res. Hum. Retroviruses* **7**, 831–838 (1991).
30. Krachmarov, C. *et al.* Antibodies that are cross-reactive for human immunodeficiency virus type 1 clade A and clade B V3 domains are common in patient sera from Cameroon, but their neutralization activity is usually restricted by epitope masking. *J. Virol.* **79**, 780–790 (2005).
31. Krachmarov, C.P., Kayman, S.C., Honnen, W.J., Trochev, O. & Pinter, A. V3-specific polyclonal antibodies affinity purified from sera of infected humans effectively neutralize primary isolates of human immunodeficiency virus type 1. *AIDS Res. Hum. Retroviruses* **17**, 1737–1748 (2001).
32. Vogel, T., Kurth, R. & Norley, S. The majority of neutralizing Abs in HIV-1-infected patients recognize linear V3 loop sequences. Studies using HIV-1MN multiple antigenic peptides. *J. Immunol.* **153**, 1895–1904 (1994).
33. Zolla-Pazner, S. Improving on nature: focusing the immune response on the V3 loop. *Hum. Antibodies* **14**, 69–72 (2005).

34. Scheid, J.F. *et al.* Broad diversity of neutralizing antibodies isolated from memory B cells in HIV-infected individuals. *Nature* **458**, 636–640 (2009).
35. Gorny, M. & Zolla-Pazner, S. Human monoclonal antibodies that neutralize HIV-1. in *HIV Immunology and HIV/SIV Vaccine Databases 2003* (eds. Korber, B. *et al.*) 37–51 (Los Alamos National Laboratory, Los Alamos, New Mexico, USA, 2003).
36. Gorny, M.K. *et al.* Preferential use of the VH5–51 gene segment by the human immune response to code for antibodies against the V3 domain of HIV-1. *Mol. Immunol.* **46**, 917–926 (2009).
37. Corti, D. *et al.* Analysis of memory B cell responses and isolation of novel monoclonal antibodies with neutralizing breadth from HIV-1-infected individuals. *PLoS One* **5**, e8805 (2010).
38. Binley, J.M. *et al.* Comprehensive cross-clade neutralization analysis of a panel of anti-human immunodeficiency virus type 1 monoclonal antibodies. *J. Virol.* **78**, 13232–13252 (2004).
39. Li, M. *et al.* Human immunodeficiency virus type 1 env clones from acute and early subtype B infections for standardized assessments of vaccine-elicited neutralizing antibodies. *J. Virol.* **79**, 10108–10125 (2005).
40. Gorny, M.K. *et al.* Cross-clade neutralizing activity of human anti-V3 monoclonal antibodies derived from the cells of individuals infected with non-B clades of HIV-1. *J. Virol.* **80**, 6865–6872 (2006).
41. Pantophlet, R., Aguilar-Sino, R.O., Wrin, T., Cavacini, L.A. & Burton, D.R. Analysis of the neutralization breadth of the anti-V3 antibody F425–B4e8 and re-assessment of its epitope fine specificity by scanning mutagenesis. *Virology* **364**, 441–453 (2007).
42. Hioe, C.E. *et al.* Anti-V3 monoclonal antibodies display broad neutralizing activities against multiple HIV-1 subtypes. *PLoS One* **5**, e10254 (2010).
43. Walker, L.M. *et al.* Broad and potent neutralizing antibodies from an African donor reveal a new HIV-1 vaccine target. *Science* **326**, 285–289 (2009).
44. Javaherian, K. *et al.* Broadly neutralizing antibodies elicited by the hypervariable neutralizing determinant of HIV-1. *Science* **250**, 1590–1593 (1990).
45. Zolla-Pazner, S. *et al.* Focusing the immune response on the V3 loop, a neutralizing epitope of the HIV-1 gp120 envelope. *Virology* **372**, 233–246 (2008).
46. Law, M., Cardoso, R.M., Wilson, I.A. & Burton, D.R. Antigenic and immunogenic study of membrane-proximal external region-grafted gp120 antigens by a DNA prime-protein boost immunization strategy. *J. Virol.* **81**, 4272–4285 (2007).
47. Zolla-Pazner, S. *et al.* Cross-clade neutralizing antibodies against HIV-1 induced in rabbits by focusing the immune response on a neutralizing epitope. *Virology* **392**, 82–93 (2009).
48. Burke, B. *et al.* Neutralizing antibody responses to subtype B and C adjuvanted HIV envelope protein vaccination in rabbits. *Virology* **387**, 147–156 (2009).
49. Haynes, B.F. *et al.* Analysis of HIV-1 subtype B third variable region peptide motifs for induction of neutralizing antibodies against HIV-1 primary isolates. *Virology* **345**, 44–55 (2006).
50. Gorny, M.K. *et al.* Neutralization of diverse human immunodeficiency virus type 1 variants by an anti-V3 human monoclonal antibody. *J. Virol.* **66**, 7538–7542 (1992).
51. Conley, A.J. *et al.* Neutralization of primary human immunodeficiency virus type 1 isolates by the broadly reactive anti-V3 monoclonal antibody, 447–52D. *J. Virol.* **68**, 6994–7000 (1994).
52. Wu, L. *et al.* Cross-clade recognition and neutralization by the V3 region from clade C human immunodeficiency virus-1 envelope. *Vaccine* **24**, 4995–5002 (2006).
53. Gorny, M.K. *et al.* Identification of a new quaternary neutralizing epitope on human immunodeficiency virus type 1 map to a common region of the V2 domain of gp120 and differ only at single positions from the clade B consensus sequence. *J. Virol.* **81**, 1424–1432 (2007).
55. Zwart, G. *et al.* Immunodominance and antigenic variation of the principal neutralization domain of HIV-1. *Virology* **181**, 481–489 (1991).
56. Zolla-Pazner, S. *et al.* The cross-clade neutralizing activity of a human monoclonal antibody is determined by the GPGR V3 motif of HIV type 1. *AIDS Res. Hum. Retroviruses* **20**, 1254–1258 (2004).
57. Gorny, M.K. *et al.* The v3 loop is accessible on the surface of most human immunodeficiency virus type 1 primary isolates and serves as a neutralization epitope. *J. Virol.* **78**, 2394–2404 (2004).
58. Gorny, M.K. *et al.* Production of site-selected neutralizing human monoclonal antibodies against the third variable domain of the human immunodeficiency virus type 1 envelope glycoprotein. *Proc. Natl. Acad. Sci. USA* **88**, 3238–3242 (1991).
59. Hennecke, J., Sebbel, P. & Glockshuber, R. Random circular permutation of DsbA reveals segments that are essential for protein folding and stability. *J. Mol. Biol.* **286**, 1197–1215 (1999).
60. Iwakura, M., Nakamura, T., Yamane, C. & Maki, K. Systematic circular permutation of an entire protein reveals essential folding elements. *Nat. Struct. Biol.* **7**, 580–585 (2000).
61. Nakamura, T. & Iwakura, M. Circular permutation analysis as a method for distinction of functional elements in the M20 loop of *Escherichia coli* dihydrofolate reductase. *J. Biol. Chem.* **274**, 19041–19047 (1999).
62. Pinter, A. Roles of HIV-1 Env variable regions in viral neutralization and vaccine development. *Curr. HIV Res.* **5**, 542–553 (2007).

ONLINE METHODS

Fab production and purification. The generation and production of all the mAbs used here have been previously described^{12,40,63}. Briefly, peripheral blood mononuclear cells from HIV-1-infected individuals were transformed by Epstein-Barr virus and cultured for 3 weeks, and the supernatants were screened by ELISA for binding to V3 peptides or V3 fusion proteins. Cells from positive cultures were then fused to a human/mouse heteromyeloma cell line, SHM-D33. The resulting heterohybridoma-expressing mAbs were repeatedly cloned to monoclonality. To obtain the Fab fragments, the selected IgGs were digested with papain in 100 mM Tris, pH 6.5, with 1 mM cysteine hydrochloride and 4 mM EDTA. The mixture was incubated at 37 °C for ~1 h, and the digestion was stopped by adding iodoacetamide to a final concentration of 10 mM. Fab and Fc fragments in the digestion mixture were separated by protein A Sepharose chromatography, and the Fab fragments collected in the flow-through were further purified by size-exclusion chromatography.

Crystallization, data collection, structure determination and refinement. The purified Fabs were mixed with several-fold excess of commercially synthesized V3 peptides selected by binding affinities measured using ELISA (see below), with lengths ranging from 20 to 25 residues (**Supplementary Table 1**). The Fab-peptide mixtures were then concentrated for crystallization by hanging drop methods. The crystallization conditions were first searched using factorial screening and then optimized by refined scanning. Suitable crystals were transferred to Brookhaven National Laboratory and flash-frozen in liquid nitrogen. X-ray diffraction data were collected at beamlines X4A, X4C and X6A of the National Synchrotron Light Sources. All datasets were integrated, indexed and scaled using HKL2000 (ref. 64).

The structures were determined by molecular replacement using Fab models selected from the PDB by BLAST⁶⁵ using sequences of the variable domains of the antibodies or models available in the laboratory. The structures were refined with CNS⁶⁶ or REFMAC⁶⁷ and manually adjusted with O⁶⁸ or Coot⁶⁹.

Design of the mimotope peptide. The database of protein 3D structures (PDB) was scanned for polypeptide chain segments of varying lengths that would match the termini of the V3 strands. A close 4-residue long match was found in the structure of pantothenate kinase (PDB 2I7P⁷⁰). The stability of the linker turn was confirmed by energy minimization. Disulfide-bridged termination replacing the original GPG turn was selected by energy minimization of multiple alternative peptides until a low-strain variant was found. All structure searches, peptide construction, and minimizations were performed using ICM⁷¹.

63. Gorny, M.K., Gianakakos, V., Sharpe, S. & Zolla-Pazner, S. Generation of human monoclonal antibodies to human immunodeficiency virus. *Proc. Natl. Acad. Sci. USA* **86**, 1624–1628 (1989).
64. Otwinowski, Z. & Minor, W. Processing of X-ray diffraction data collected in oscillation mode. *Methods Enzymol.* **276**, 307–326 (1997).
65. Altschul, S.F., Gish, W., Miller, W., Myers, E.W. & Lipman, D.J. Basic local alignment search tool. *J. Mol. Biol.* **215**, 403–410 (1990).
66. Brunger, A.T. *et al.* Crystallography & NMR system: A new software suite for macromolecular structure determination. *Acta Crystallogr. D Biol. Crystallogr.* **54**, 905–921 (1998).
67. Murshudov, G.N., Vagin, A.A. & Dodson, E.J. Refinement of macromolecular structures by the maximum-likelihood method. *Acta Crystallogr. D Biol. Crystallogr.* **53**, 240–255 (1997).
68. Jones, T.A., Zou, J.Y., Cowan, S.W. & Kjeldgaard, M. Improved methods for building protein models in electron density maps and the location of errors in these models. *Acta Crystallogr. A* **47**, 110–119 (1991).
69. Emsley, P. & Cowtan, K. Coot: model-building tools for molecular graphics. *Acta Crystallogr. D Biol. Crystallogr.* **60**, 2126–2132 (2004).
70. Hong, B.S. *et al.* Crystal structures of human pantothenate kinases. Insights into allosteric regulation and mutations linked to a neurodegeneration disorder. *J. Biol. Chem.* **282**, 27984–27993 (2007).
71. Abagyan, R.A., Totrov, M. & Kuznetsov, D. ICM - A new method for protein modeling and design: applications to docking and structure prediction from the distorted native conformation. *J. Comput. Chem.* **15**, 488–506 (1994).